

2 **Characterization and sorting of cells based on stiffness contrast in**
3 **a microfluidic channel**

4 P. Sajeesh¹, A. Raj¹, M. Doble², A. K. Sen^{1,*}

5 ¹*Department of Mechanical Engineering, Indian Institute of Technology Madras, Chennai-600036, India*

6 ²*Department of Biotechnology, Indian Institute of Technology Madras, Chennai-600036, India*

7

8 *Author to whom correspondence should be addressed. Email: ashis@iitm.ac.in

9

10 ***S.1 Cell culture protocol***

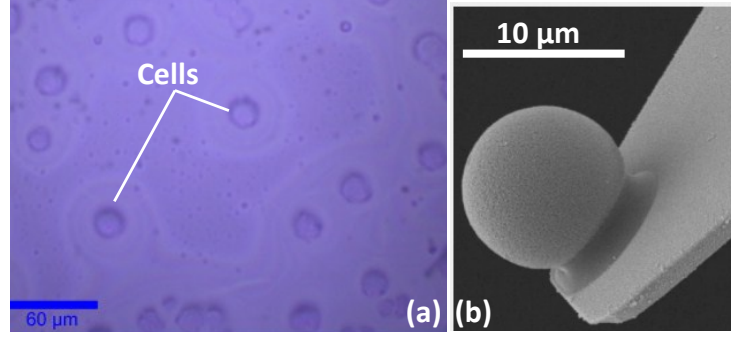
11 The cell lines (National Centre for Cell Sciences, Pune, India) kept at -80 °C were revived, cultured into T-25
12 flask in Dulbecco's Modified Eagle Medium (DMEM) (Himedia, India), which contained 20% fetal bovine
13 serum and antibiotic mix (50 mg gentamicin, 100 mg streptomycin, and 62.77 mg penicillin), and the cells were
14 incubated in CO_2 incubator. When the cells were grown to confluence, the media was removed and the cells
15 were washed thrice with Phosphate Buffered Saline. Then, PBS was removed completely and trypsinized with
16 1X trypsin and incubated for 2-3 min in CO_2 incubator. The trypsinized cells were added with 1.0 mL DMEM
17 and then transferred into 15 mL Falcon tube and centrifuged for 5 min at 1800 rpm. The supernatant was
18 removed and 1.0 mL of fresh media was added to the pellet and the cells were gently re-suspended. Then, the
19 cells were sorted out to a size of 25 μm using Fluorescence Activated Cell Sorting (FACS ARIA III). Cells of
20 this size were sorted out using polystyrene beads of same size as the standard. For tagging, cells were
21 transferred into falcon tube, centrifuged and pellet was taken. 1-2 mL of Rhodamine was added to this pellet and
22 centrifuged again after 5 min. Supernatant was discarded and pellets are washed with fresh media. The process
23 was continued until the cells were tagged up to the required level (distinguishable from non-tagged cells).

24 ***S.2 Cell Immobilization protocol***

25 First, Poly-D-Lysine solution was mixed with autoclaved PBS to achieve the desired pH of 7.4. Then, the
26 mixture was placed on a glass slide and allowed to dry for 90 min. Cultured cells are then seeded on to the glass
27 slide, coated with Poly-D-Lysine. During the drying process, most of the cells are immobilized onto the glass
28 slide. Next, the glass slide was rinsed with sterile DI water thrice to remove the remaining cells, which were not
29 immobilized properly and remove the cell medium in which the cells were cultured. Further, the glass slide was
30 dried in the sterile hood for 40 min. Cell sample is required to be immobilized in this way for loading the cells
31 on the AFM stage for the nanoindentation experiments. An image of the immobilized cell sample captured by
32 the inverted optical stage of AFM is shown in Fig. S1(a).

33 ***S.3 Selection of the cantilever probe***

34 If the cantilever probe is too stiff, smaller deflection of the probe can damage the cell during the indentation
35 experiments, whereas, if the cantilever is too soft, probe would not make proper indentation on the cells to
36 obtain the correct Young's modulus E_c . Moderate range of indentations on cells are possible with colloidal AFM
37 probes (cantilever probe with spherical bead at the tip) without any puncturing and local straining of cells¹ to
38 obtain average value of Young's modulus.



39

40 Fig. S1 (a) Image of the immobilized cell (HL 60 cell) on glass slide using Poly-L-Lysine (b) SEM image of the
41 AFM colloidal probe used in our studies.

42 S.4 AFM data analysis

43 From the AFM measurement data, clean deflection versus indentation curves with flat pre-contact region and a
44 post contact region were considered for the data analysis by fitting with the Hertzian elastic model (Hertz 1882).
45 Additional interaction between cell sample and probe including the Van der Waals interaction and adhesive
46 forces cannot not be accounted by the Hertz model². Thus from the nanoindentation experiments, only the
47 loading data which is free from these additional interactions are used for fitting the model. None of the
48 unloading data was used for our analysis. Hertz model assumes that the indentation on the cell line is negligible
49 in comparison to the thickness of the sample³. So we used a maximum indentation which is 10% of the cell size.
50 A maximum indentation depth of 1000 nm was set in our experiments. We have assumed the cell-probe
51 interaction as linear elastic, which is valid since the hysteresis between the loading and unloading curves is
52 relatively small². The smaller hysteresis is due to the lower viscous dissipation which occurs because of lower
53 indentation range, smaller loading rate (400 nm/s) and absence of any liquid medium around the cell
54 (indentation experiment is performed with air as medium)⁴. Hertz model is appropriate if the indentation is
55 performed with a colloidal probe having a spherical bead at the tip³, which prevents the variation in Young's
56 modulus. Moreover Hertz model is widely used in literature for fitting data in case of nanoindentation
57 experiments (using AFM) with cells.

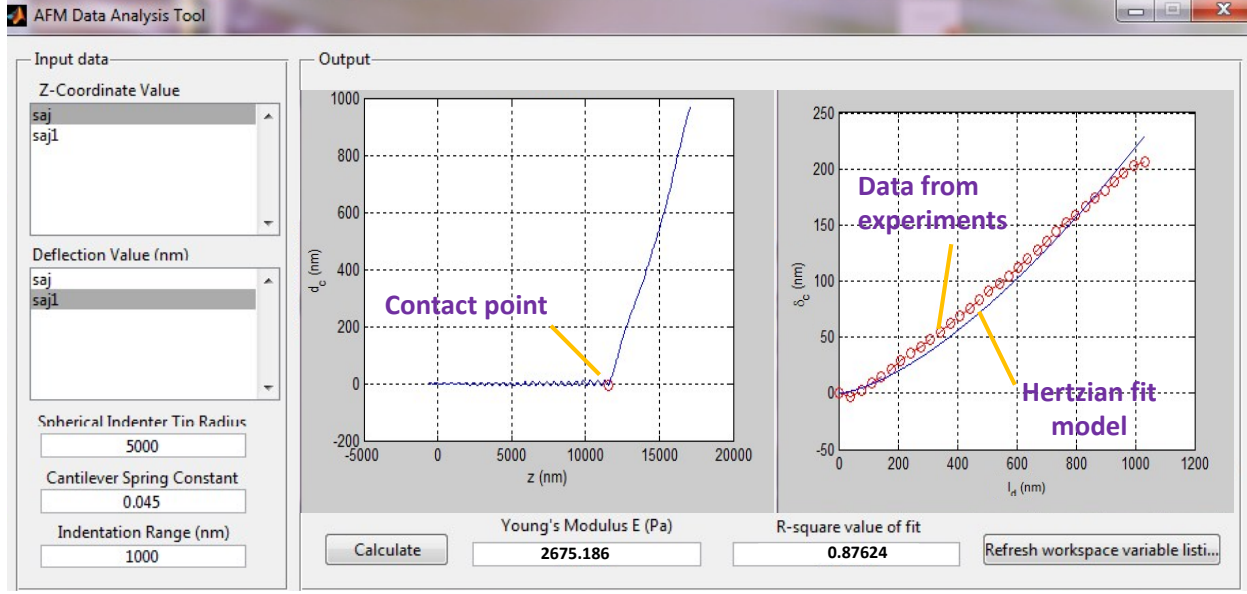
58 First, the deflection (d_c) versus piezo position (Z) data, for the data points Z within the maximum specified
59 indentation, was smoothed using a cubic spline fit. Next, the precise contact point was determined with the help
60 of a custom made MATLAB code (as described in the next section). A trial contact point (Z_{0i}) was selected
61 randomly; a linear fit was performed on the data to the left side and a Hertzian fit was performed on the data to
62 the right of the initial selected contact point. Then, different trial contact points were selected and at each trial
63 contact point, the aggregate mean square error (MSE) for both the fits were calculated. Out of all the selected
64 trial contact points (Z_{0i}), the trial point which provides minimum aggregate MSE was selected as the accurate
65 contact point Z_0 . The deflection of the cantilever at this contact point Z_0 is denoted by d_0 . So, the indentation
66 on the cell is calculated using $I_d = z - z_0 - (d_c - d_0)$. The force acting on the cantilever is calculated as the
67 product of the relative deflection $\delta_c = (d_c - d_0)$ and the spring constant k of the cantilever. Finally, elastic
68 modulus of cell line E_c is found out by fitting F versus I_d curve with the Hertz model (Hertz1882) (as shown in
69 the Eqn. below) in lower indentation range to avoid the nonlinear elastic effects of the cells,

70

$$F = \frac{4}{3} \frac{E_c}{1 - \nu^2} \sqrt[3]{R_t I_d^3} \quad (S1)$$

71 where R_t is the radius of the spherical tip of colloidal probe and ν is the Poisson's ratio of the cell. A Poisson
72 ratio of 0.5 is usually considered for lipid bilayers, cells and vesicles (Radmacher 2007, Liang 2004). Since the
73 size of the cells is more than $10 \mu m$, the ratio of the bending force to elastic force on the cell is less than 0.05.

74 Thus, the small bending deformation of cell line can be ignored (Lulevich 2006) during the indentation
 75 experiments.



76

77 Fig. S2 Output window of the GUI “AFMTOOL”, piezo position vs. deflection curve obtained from the
 78 indentation experiment (left), identified contact point is shown by red circle, analysed indentation I_d vs. relative
 79 deflection δ_c profile for HL60 cell line (right). Experimental data obtained from the AFM data analysis is shown
 80 as points and the Hertzian fit on the data is shown by solid curve.

81 S. 5 Design of the device

82 S.5.1 Focusing and spacing control module.

83 We have checked the number density of cells in a sample in-situ during the experiments. Initial spacing
 84 between the cells can be controlled by adjusting the cell concentration to ensure that the objects are well isolated
 85 (minimum gap maintained) prior to entering the sensing channel of the sorting module. After capturing the
 86 trajectory of objects in the sensing channel, if the required spacing between objects is not attained, it is possible
 87 to achieve this by increasing the sheath fluid flow rate (increasing the spacing control flow rate ratio f_{sc}).
 88

89 If we adjust the sheath-to-sample flow rate ratio f_p such that the dividing streamline that separates the sheath
 90 fluid from the sample fluid is located at a distance equal to the size of cells D_d in the sample, then all the cells
 91 will be well focused to that side wall. The flow rate ratio $f_p = q/Q$ required for focusing all cells in the sample to
 92 one of the side walls can be found out from the following correlation (detailed derivation is shown elsewhere ⁵),

$$93 \quad \rho(1 + f_p) - 1 + \sum_{n=odd}^{\infty} \frac{96 \alpha f_p}{\pi^5 n^5} [C(B-1) - A] - \sum_{n=odd}^{\infty} \frac{96 \alpha}{\pi^5 n^5} [A - C(1+B)] = 0 \quad (S2)$$

94 where $\alpha = \frac{H}{W_0}$ is the aspect ratio of the channel, ρ is the size ratio of the cells in the sample, $A = \sinh\left(\frac{n\pi\rho}{\alpha}\right)$,
 95 $B = \cosh\left(\frac{n\pi\rho}{\alpha}\right)$ and $C = \tanh\left(\frac{n\pi}{2\alpha}\right)$. The eqn. (2) is solved numerically (using MATLAB) to find out the
 96 required flow rate ratio f_p .

97 S.5.2 Sorting module.

98 The schematic diagram of the sorting module is shown in Fig. S3(a). Main channel flow rate in the sorting
 99 module is divided into straight branch channel flow rate Q_{st} and side branch channel flow rate Q_{st} . Fluid

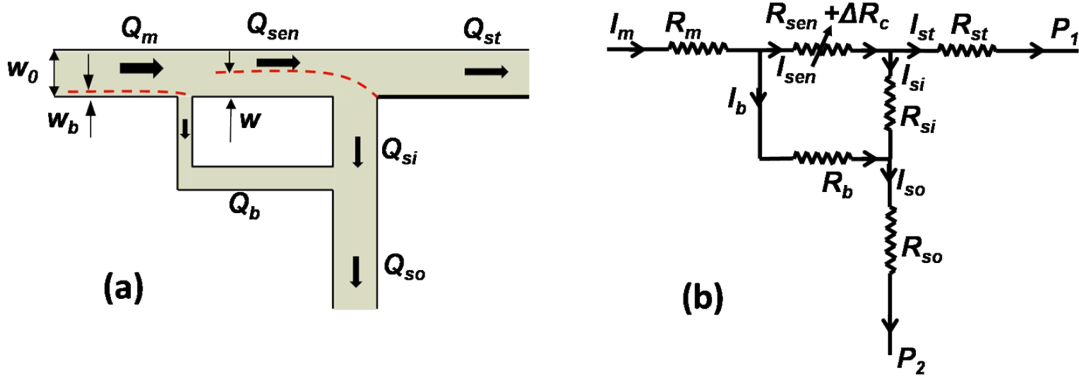
100 streams entering these channels from the main channel separated by a “dividing streamline”. The distance
 101 between the dividing streamline from one of the side wall is called the “critical stream width w ”. Initial critical
 102 stream width w_0 is determined by the initial flow rate ratio r^i (ratio of flow rates in the straight branch Q_{st} to the
 103 side branch Q_{si}) in the absence of object in the sensing channel. This initial flow rate ratio and thus the critical
 104 stream width w changes depending on the resistance offered by the objects reaches at the sensing channel.

105 An equivalent electrical circuit of sorting module is shown in Fig. S3(b). Usage of Kirchhoff’s law to find out
 106 the equivalent resistance network and circuit analogy to derive the expressions for the flow rates at the branch
 107 channel and the side branch which is separated from the sensing channel is explained elsewhere⁵. Finally the
 108 both flow rates are combined to find out the expression for the critical stream width w in the sensing channel as
 109 follows,

$$110 \quad W_0 - w(l+r) + \sum_{n=odd}^{\infty} \frac{96 H r}{\pi^5 n^5} [G(F-l) - E] + \sum_{n=odd}^{\infty} \frac{96 H}{\pi^5 n^5} [E - G(l+F)] = 0 \quad (S3)$$

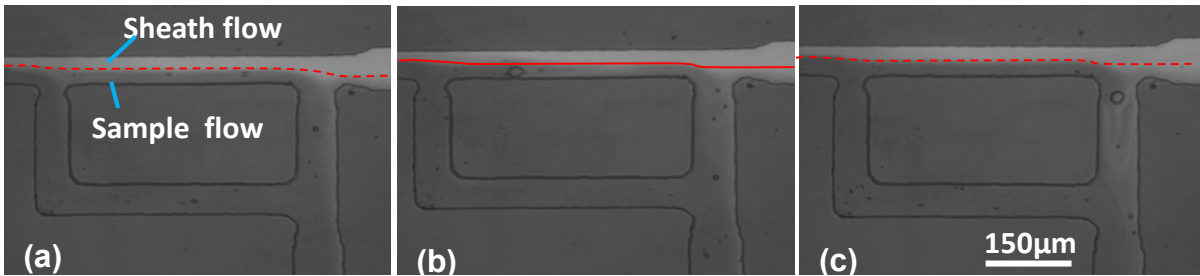
111 where $r = Q_{st}/Q_{si}$ is the ratio of the flow rate in the straight branch channel to the side branch channel, W_0 is the
 112 width of the sensing channel, H is the height of the channel, $E = \sinh\left(\frac{n\pi w}{H}\right)$, $F = \cosh\left(\frac{n\pi w}{H}\right)$ and

$$113 \quad G = \tanh\left(\frac{n\pi W_0}{2H}\right).$$



114

115 **Fig. S3** (a) Schematic diagram of the sorting module depicting the relative flow rates in different channel
 116 sections (b) Equivalent resistance network of the sorting module, resistance in the sensing channel is variable
 117 resistance $R_{sen} + \Delta R_c$



118

119

120 **Fig. S4** Experimental images showing shifting of interface in the sensing channel (a) no cell present inside the
 121 sensing section (b) cell is present in the sensing section (c) cell leaving the sensing section.

122

123 **References**

- 124 1 E. K. Dimitriadis, F. Horkay, J. Maresca, B. Kachar and R. S. Chadwick, *Biophys. J.*, 2002, **82**, 2798–
125 810.
- 126 2 B. Cappella and G. Dietler, *Surf. Sci. Rep.*, 1999, **34**, 1–104.
- 127 3 H.-J. Butt, B. Cappella and M. Kappl, *Surf. Sci. Rep.*, 2005, **59**, 1–152.
- 128 4 Q. S. Li, G. Y. H. Lee, C. N. Ong and C. T. Lim, *Biochem. Biophys. Res. Commun.*, 2008, **374**, 609–13.
- 129 5 P. Sajeesh, S. Manasi, M. Doble and a K. Sen, *Lab Chip*, 2015, **15**, 3738–48.